Inorg. Chem. **2007**, *46*, 5361–5371

Elucidation of the Solution Structure and Water-Exchange Mechanism of Paramagnetic $[Fe^{II}(edta)(H_2O)]^{2-}$

Joachim Maigut, Roland Meier, Achim Zahl, and Rudi van Eldik*

Institute for Inorganic Chemistry, University of Erlangen−Nürnberg, Egerlandstrasse 1, 91058 Erlangen, Germany

Received March 12, 2007

The lability and structural dynamics of $[Fe^{II}(edta)(H_2O)]^{2-}$ (edta = ethylenediaminetetraacetate) in aqueous solution strongly depend on solvent interactions. To study the solution structure and water-exchange mechanism, ^{1}H, ^{13}C, and ^{17}O NMR techniques were applied. The water-exchange reaction was studied through the paramagnetic effect of the complex on the relaxation rate of the ^{17}O nucleus of the bulk water. In addition to variable-temperature experiments, high-pressure NMR techniques were applied to elucidate the intimate nature of the water-exchange mechanism. The water molecule in the seventh coordination site of the edta complex is strongly labilized, as shown by the water-exchange rate constant of $(2.7 \pm 0.1) \times 10^6$ s^{-1} at 298.2 K and ambient pressure. The activation parameters $\Delta H^{\neq}$, $\Delta S^{\neq}$, and $\Delta V^{\neq}$ were found to be 43.2 ± 0.5 kJ mol^{-1}, +23 ± 2 J K^{-1} mol^{-1}, and +8.6 ± 0.4 cm^3 mol^{-1}, respectively, in line with a dissociatively activated interchange (I_d) mechanism. The scalar coupling constant (A/h) for the Fe^{II}–O interaction was found to be 10.4 MHz, slightly larger than the value A/h = 9.4 MHz for this interaction in the hexa-aqua Fe^{II} complex. The solution structure and dynamics of $[Fe^{II}(edta)(H_2O)]^{2-}$ were clarified by ^{1}H and ^{13}C NMR experiments. The complex undergoes a Δ,Λ-isomerization process with interconversion of in-plane (IP) and out-of-plane (OP) positions. Acetate scrambling was also found in an NMR study of the corresponding NO complex, $[Fe^{III}(edta)(NO^-)]^{2-}$.

Introduction

In 1993, Mizuta et al.[1,2] reported the first crystal structure of the Fe^{II}−edta complex. Aside from the hexadentate edta (ethylenediaminetetraacetate) chelate, a water molecule was detected at the seventh coordination site of the metal center. Since that finding, the seven-coordinate edta complex is commonly expressed by the formula $[Fe^{II}(edta)(H_2O)]^{2-}$. Surprisingly, dried crystals were found to be stable against oxidation, in contrast to the extremely oxygen-sensitive solution of this complex.[1]

The observed difference in reactivity reflects the important contribution of the solvent in describing the substitution and redox behavior of this complex. A detailed study of the kinetics of the oxidation of $[Fe^{II}(edta)(H_2O)]^{2-}$ by dioxygen in aqueous solution revealed that the oxidation necessarily proceeds via the substitution of the labile water molecule by molecular oxygen. Once the dioxygen species $[Fe^{II}(edta)O_2]^{2-}$ is formed, electron transfer leads to the Fe^{III}-superoxide species, followed by dimerization, and finally splitting of the dimer to give the oxidation product $[Fe^{III}(edta)(H_2O)]^-$,[3,4] which is again a seven-coordinate species.

$$[Fe^{II}(edta)(H_2O)]^{2-} + O_2 \rightleftharpoons [Fe^{II}(edta)(O_2)]^{2-} + H_2O$$

$$[Fe^{II}(edta)(O_2)]^{2-} \rightarrow [Fe^{III}(edta)(O_2^-)]^{2-}$$

$$[Fe^{III}(edta)(O_2^-)]^{2-} + [Fe^{II}(edta)(H_2O)]^{2-} \rightarrow [(edta)Fe^{III}-(\mu\text{-}O_2^{2-})-Fe^{III}(edta)]^{4-} + H_2O$$

$$[(edta)Fe^{III}-(\mu\text{-}O_2^{2-})-Fe^{III}(edta)]^{4-} + 2H^+ + 2H_2O \rightarrow 2[Fe^{III}(edta)(H_2O)]^- + H_2O_2$$

Therefore, the water molecule in the seventh coordination site plays a crucial role in describing the chemistry of $[Fe^{II}(edta)(H_2O)]^{2-}$ because this complex gained interest in

* To whom correspondence should be addressed. E-mail: vaneldik@chemie.uni-erlangen.de.

(1) Mizuta, T.; Wang, J.; Miyoshi, K. *Bull. Chem. Soc. Jpn.* **1993**, *66*, 2547.
(2) Mizuta, T.; Wang, J.; Miyoshi, K. *Inorg. Chim. Acta* **1995**, *230*, 119.
(3) Zang, V.; van Eldik, R. *Inorg. Chem.* **1990**, *29*, 1705.
(4) Seibig, S.; van Eldik, R. *Inorg. Chem.* **1997**, *36*, 4115.

10.1021/ic700472q CCC: $37.00
Published on Web 05/27/2007

industrial[5−11] and medical[12] applications as a result of its excellent NO-scavenging properties in aqueous media. Aqueous solutions of $[Fe^{II}(edta)(H_2O)]^{2-}$ as scrubber liquid in the BioDeNO$_x$ process for NO removal from flue gases is a promising alternative[13] to the dry process of selective (non)-catalytic reduction (S(N)CR) that suffers from catalyst poisoning. In the wet denitrification process, the absorption of poorly water soluble NO (1.25×10^{-3} M atm^{-1} at 50 °C) in the aqueous phase requires $[Fe^{II}(edta)(H_2O)]^{2-}$ to reversibly bind NO. The edta complex is of particular interest as an absorption catalyst because of a fast NO-uptake rate constant of $(2.4 \pm 0.1) \times 10^8$ M^{-1} s^{-1} and a high stability constant of $(2.1 \pm 0.2) \times 10^6$ M^{-1} at 25 °C.[14]

$$[Fe^{II}(edta)(H_2O)]^{2-} + NO \rightleftharpoons [Fe^{III}(edta)(NO^-)]^{2-} + H_2O$$

Analogous to the oxidation by dioxygen, nitrosylation proceeds via the substitution of coordinated water by NO, followed by subsequent electron transfer to form the Fe^{III}−NO$^-$ complex.

Investigation of the displacement of a coordinated water molecule by an entering bulk water molecule and the underlying intimate substitution mechanism is therefore of importance in understanding the reactivity of $[Fe^{II}(edta)(H_2O)]^{2-}$ because the described reactions have to proceed via substitution of the bound water molecule. However, the structure of $[Fe^{II}(edta)(H_2O)]^{2-}$ in aqueous solution was never studied, nor was the kinetics for the water-exchange reaction because solutions of this complex are extremely oxygen sensitive. Especially, the water-exchange mechanism will reveal information on steric constraints around the metal center and on labilizing effects due to the chelate ligand.

According to Langford and Gray,[15] substitution processes can generally be classified with respect to the degree of bond making and bond breaking along the reaction coordinate to the transition state. Aside from the two limiting cases, complete dissociation of the bound ligand (D mechanism), and association of the entering ligand (A mechanism), an interchange mechanism is possible. Within the category for interchange mechanisms, a continuum of transition states is possible as the degree of bond making with the entering ligand can range from substantial (I_a, associative interchange) to negligible (I_d, dissociative interchange). The entering and leaving water molecules have substantial bonding to the metal center in an associatively activated interchange (I_a) process, whereas a dissociatively activated interchange (I_d) process involves weak bond making of the entering solvent and weak bonding of the leaving solvent molecule. Temperature-dependent measurements of the exchange-rate yield the activation enthalpy, $\Delta H^{\neq}$, and activation entropy, $\Delta S^{\neq}$, from which limited mechanistic conclusions can be drawn. In recent years the assignment of solvent-exchange mechanisms is mainly based on variable-pressure experiments.[16] The detection of pressure-induced changes in the exchange rate allows the determination of the activation volume, $\Delta V^{\neq}$, which is a composite of intrinsic, $\Delta V^{\neq}_{intr}$, and solvational, $\Delta V^{\neq}_{solv}$, contributions and simplifies to $\Delta V^{\neq} \approx \Delta V^{\neq}_{intr}$ because $\Delta V^{\neq}_{solv}$ is small and negligible in the case of water-exchange reactions. The activation volume is a potent tool in the determination of reaction mechanisms as it unambiguously connects the intimate mechanism with the sign of $\Delta V^{\neq}$, namely for associatively activated processes $\Delta V^{\neq} < 0$ and for dissociatively activated processes $\Delta V^{\neq} > 0$. In a semiempirical model developed by Swaddle and Mak.,[17,18] the limiting activation volume for di- and trivalent 3d transition-metal−aqua cations was estimated to be $\Delta V^{\neq}_{limit} = +13.5$ cm^3 mol^{-1} for a D mechanism and -13.5 cm^3 mol^{-1} for an A mechanism. With these limiting values, a guideline exists from which a limiting mechanism can be concluded, even if evidence for an intermediate of higher or lower coordination number does not exist.

Aside from the exchange kinetics, the solution structure and dynamics of the complex in aqueous media can be investigated by NMR techniques. For some complexes with edta and edta-type ligands, namely, Al^{III}−edta, Ga^{III}−edta,[19] and Co^{II}−edta,[20] a rapid interchange of the acetate groups between axial (out-of-plane, (OP)) and equatorial (in-plane, (IP)) positions was found in water (i.e., Δ,Λ isomerization).[19] However, in DMSO, the Al^{III}−edta NMR spectra no longer showed the averaged signals as a result of blocked acetate interchange as compared to aqueous media. The observed resonance-^{1}H NMR pattern for Al^{III}−edta in DMSO is now similar to that for the inert Co^{III}−edta with four signals (two AB spin systems) for the nonequivalent methylene protons of the acetates in the axial and equatorial positions and one AA′BB′ spectrum of the ethylenediamine unit. Therefore, the interchange rate of the acetate groups and consequently the Δ,Λ-isomerization process need to be considered as strongly solvent dependent. For the Fe^{II}−edta system, it has not been clarified so far whether the Δ,Λ-isomerization process occurs or whether it adopts a static structure in solution.

The reactivity and structural dynamics of $[Fe^{II}(edta)(H_2O)]^{2-}$ in solution are strongly related to solvent interactions. To

(5) Sada, E.; Kumazawa, H.; Takada, H. *Ind. Eng. Chem. Fundam.* **1984**, *23*, 60.
(6) Sada, E.; Kumazawa, H.; Hikosaka, H. *Ind. Eng. Chem. Fundam.* **1986**, *25*, 286.
(7) Sada, E.; Kumazawa, H.; Machida, H. *Ind. Eng. Chem. Res.* **1987**, *26*, 2016.
(8) Littlejohn, D.; Chang, S. G. *J. Phys. Chem.* **1982**, *86*, 537.
(9) Chang, S. G.; Litteljohn, D.; Lynn, S. *Environ. Sci. Technol.* **1983**, *17*, 649.
(10) Demmink, J. F.; van Gils, I. C. F.; Beenackers, A. A. C. M. *Ind. Eng. Chem. Res.* **1997**, *36*, 4914.
(11) Tsai, S.; Bedell, S. A.; Kirby, L. H.; Zabcik, D. *J. Environ. Prog.* **1989**, *8*, 126.
(12) Shepherd, R. E.; Sweetland, M. A.; Junker, D. E. *J. Inorg. Biochem.* **1997**, *65*, 1.
(13) van der Maas, P.; van den Brink, P.; Utomo, S.; Klapwijk, B.; Lens, P. *Biotechnol. Bioeng.* **2006**, *94*, 575.
(14) Schneppensieper, T.; Wanat, A.; Stochel, G.; van Eldik, R. *Inorg. Chem.* **2002**, *41*, 2565.
(15) *Ligand Substitution Processes*; Langford, C. N., Gray, H. B., Eds.; W. A. Benjamin: New York, 1966.
(16) *High-Pressure Chemistry*; van Eldik, R., Klärner, F.-G., Eds; Wiley-VCH: Weinheim, Germany, 2002.
(17) Swaddle, T. W.; Mak, M. K. S. *Can. J. Chem.* **1981**, *36*, 89.
(18) Swaddle, T. W. *Adv. Inorg. Bioinorg. Mech.* **1983**, *2*, 95.
(19) Jung, W. S.; Chung, Y. K.; Shin, D. M.; Kim, S. D. *Bull. Chem. Soc. Jpn.* **2002**, *75*, 1263.
(20) Everhart, D. S.; Evilia, R. F. *Inorg. Chem.* **1977**, *16*, 120.

clarify the solution structure and water-exchange mechanism, ^1H, ^{13}C, and variable-temperature and -pressure ^{17}O NMR studies were performed in this investigation.

Experimental Section

Materials. The reagents used in this investigation were all of analytical grade. The NMR spectra for the H_4−edta ligand (Acros Organics) in D_2O/NaOD revealed no significant impurities aside from the resonances of the compound, and the chelate was therefore used as supplied without any further purification. ^1H NMR: δ 3.30 (s, 4H, $-N-CH_2-CH_2-N-$), 3.68 (s, 8H, $-N-CH_2-COO^-$). ^{13}C NMR: δ 53.81 (2C, $-N-CH_2-CH_2-N-$), 60.23 (4C, $-N-CH_2-COO^-$), 176.58 (4C, $-N-CH_2-COO^-$). Solutions were prepared in doubly destilled water, and the ionic strength was adjusted with $NaClO_4$ (Merck) to 0.5 M for all of the kinetic investigations. The samples for the water-exchange measurements were prepared by dissolving the ligand in 0.1 M sodium acetate buffer solution (Fisher Chemicals). The pH was measured with a Metrohm 713 pH-Meter using a Metrohm glass electrode (filled with sodium chloride instead of potassium chloride to prevent precipitation of poorly soluble potassium perchlorate) and adjusted to pH 5.0 with NaOH (Acros Organics). The solution was deoxygenated several times under a vacuum and saturated with argon before the appropriate amount of $FeSO_4 \cdot 7H_2O$ (Acros Organics) was added. For the estimation of the exchange kinetics, the complex solution was enriched with the ^{17}O isotope by the addition of argon saturated $H_2{}^{17}O$ (10%, Deutero) using syringe techniques to give a total enrichment of 1% ^{17}O in the studied samples. To improve the signal-to-noise ratio in the ^1H and ^{13}C NMR experiments, solid $Na_2[Fe^{II}(edta)(H_2O)]$ was prepared by dissolving H_4−edta (2.92 g, Acros Organics) in doubly destilled water (10 mL). After deprotonation with 2 equiv of Na_2CO_3, a clear solution was obtained and saturated with argon. Under strict exclusion of oxygen, 2.78 g of $Fe^{II}SO_4 \cdot 7H_2O$ was added. Immediately after the addition of the Fe^{II} salt, a white precipitate of $Na_2[Fe^{II}(edta)(H_2O)]$ was obtained. The solid was filtered under nitrogen and dried under an oil-pump vacuum. For the NMR experiments, the solid complex was dissolved in an argon-saturated D_2O solution (pD 5.4). The solution species was analyzed by mass spectroscopy EI^+-MS: *m/z* (relative intensity): 360 (34%, $[M-H]^+$), 343 (67%, $[M-H_2O]^+$) (JEOL MStation JMS 700).

The nitrosyl complex, $[Fe^{III}(edta)(NO^-)]^{2-}$, was prepared by passing NO through an argon-saturated solution of 100 mM $[Fe^{II}(edta)(H_2O)]^{2-}$ (pD 5.4) in an NMR tube that was kept and sealed under an argon atmosphere. The commercially available 99.5 vol % nitric oxide (Air Liquide) was cleaned of impurities on an Ascarite II column (sodium hydroxide on silica gel, Sigma-Aldrich) and on a P_2O_5 column. The gas cylinders were filled at a maximum pressure of 20 bar to decrease the decomposition rate of nitric oxide.

^1H and ^{13}C NMR Measurements. The NMR experiments were carried out on a Bruker AVANCE DRX 400WB spectrometer at a resonance frequency of 400.13 for ^1H and 100.61 MHz for ^{13}C nuclei. To avoid oxidation throughout the measurements, NMR tubes sealed with Teflon screw caps were used in which the samples were kept under an argon atmosphere. The spectra were recorded in deuterium solvent lock (D_2O) mode and referenced against 3-(trimethylsilyl) propionic acid (TSP, $\delta = 0$ ppm). Typical acquisition parameters for ^1H experiments were pulse length, 2.4 μs (30°); relaxation delay, 2.0 s; scans, 214; sweep width, 80000 Hz. For ^{13}C NMR measurements, typical acquisition parameters were pulse length, 7.4 μs; relaxation delay, 3.0 s; scans, 22 k; sweep width, 100 000 Hz. The ^{13}C spectra were collected with a power-gated decoupling pulse sequence.

^{17}O NMR Measurements. The ^{17}O NMR spectra were recorded on a Bruker AVANCE DRX 400WB spectrometer equipped with a spectrospin superconducting wide-bore magnet operating at a resonance frequency of 54.24 MHz at a magnetic induction of 9.4 T. Measurements at atmospheric pressure were performed with a commercial 5 mm Bruker broadband probe thermostated with a Bruker B−VT 3000 variable-temperature unit. Relaxation rates and chemical shifts were measured for the paramagnetic solutions and for the aqueous buffer solution as a reference. To avoid susceptibility corrections of the measured data in the determination of the shift of the ^{17}O resonance, the sample was sealed in a 4 mm sphere fitted inside a standard NMR tube. The samples with and without the paramagnetic compound were concentrically surrounded by an external deuterated standard (toluene) for locking purposes. The chemical shifts, as well as the line width at half-height of the signal, were determined by a deconvolution procedure on the real part of the Fourier transformed spectra with a Lorentzian shape function in the data analysis module of Bruker Topspin 1.3 software. Pressure-dependent measurements were carried out with a home-made thermostated high-pressure probe.[21] The sample was measured in a standard 5 mm NMR tube cut to a length of 50 mm. To enable pressure transmittance to the solution, the NMR tube was closed with a moveable macor piston. The advantage of this method is that oxygen-sensitive samples can be easily placed in the NMR tube and sealed with the macor piston under an argon atmosphere. A safe subsequent transfer to the high-pressure probe is assured. The pressure was applied to the high-pressure probe via a perfluorated hydrocarbon (hexafluoropropyleneoxide, Hostinert 175, Hoechst) and measured by a VDO gauge with an accuracy of ±1%. Temperature was adjusted with circulating, thermostated water (Colora thermostat WK 16) to ±0.1 K of the desired value and monitored before each measurement with an internal Pt-resistance thermometer with an accuracy of ±0.2 K.

Results and Discussion

Water-Exchange Reaction. The paramagnetic high-spin Fe^{II} complex, $[Fe^{II}(edta)(H_2O)]^{2-}$, has a pronounced influence on relaxation rates of nuclei in its proximity. Aside from the enhancement of longitudinal and transverse relaxation rates, an influence on the chemical shifts of nuclei close to the paramagnetic Fe^{II} center is apparent. It is valuable that the exchange rates of solvent molecules between the bulk and the coordination site of $[Fe^{II}(edta)(H_2O)]^{2-}$ are accessible by studying relaxation rates and the resonance shift of the ^{17}O nucleus for water molecules at variable temperature and pressure. Transverse relaxation rates were determined, employing the $H_2{}^{17}O$ line-broadening technique. The obtained half-widths of the ^{17}O NMR signal of the bulk solvent in the presence ($\Delta\nu_{obs}$) and absence ($\Delta\nu_{solvent}$) of paramagnetic $[Fe^{II}(edta)(H_2O)]^{2-}$, together with the mole fraction of bound water (P_m), were used to calculate the reduced transverse relaxation rates ($1/T_{2r}$) for each temperature and pressure. According to Swift and Connick,[22,23] T_{2r} is related to the transverse relaxation time of coordinated water in the inner sphere of the complex in the absence of a chemical exchange (T_{2m}), the difference in resonance frequency of bulk solvent and solvent in the first coordination sphere ($\Delta\omega_m$), and the

(21) Zahl, A.; Neubrand, A.; Aygen, S.; van Eldik, R. *Rev. Sci. Instrum.* **1994**, *65*, 882.
(22) Swift, T. J.; Connick, R. E. *J. Chem. Phys.* **1962**, *37*, 307.
(23) Swift, T. J.; Connick, R. E. *J. Chem. Phys.* **1964**, *41*, 2553.

mean lifetime of coordinated solvent (τ_m). The exchange-rate constant between coordinated and bulk solvent, k_{ex}, can accordingly be expressed as the reciprocal residence time of the bound solvent molecule $k_{ex} = 1/\tau_m$. A summary of these relationships is given in eq 1.

$$\frac{1}{T_{2r}} = \pi\frac{1}{P_m}(\Delta\nu_{obs} - \Delta\nu_{solvent}) = \frac{1}{\tau_m}\left\{\frac{T_{2m}^{-2} + (T_{2m}\tau_m)^{-1} + \Delta\omega_m^2}{(T_{2m}^{-1} + \tau_m^{-1})^2 + \Delta\omega_m^2}\right\} + \frac{1}{T_{2os}} \quad (1)$$

The mole fraction of the solvent in the exchanging site compared to the bulk solvent, represented by the term P_m, normalizes the measured line-width difference ($\Delta\nu_{obs} - \Delta\nu_{solvent}$) to the applied-complex concentration. The difference in the resonance frequency of bulk solvent and solvent in the first coordination sphere of the iron complex is expressed by $\Delta\omega_m$. T_{2os} represents an outer-sphere contribution to T_{2r} that arises from long-range interactions of the paramagnetic unpaired electrons of the iron complex with water outside the inner coordination sphere. These possible contributions are not all observable in the studied system because of the limited temperature range. The measurements are restricted to a rather small kinetic window between the boiling and freezing points of water. Therefore, a contribution of $1/T_{2os}$ to the reduced transverse relaxation rate that would be clearly visible by a changeover to a positive slope at low temperatures was never observed. The absence of this contribution justifies the application of eq 1 in a reduced form (eq 2a), where outer-sphere contributions to relaxation are ignored. At elevated temperatures, the $[Fe^{II}(edta)(H_2O)]^{2-}$ complex showed a small contribution from $1/T_{2m}$. To evaluate the derived activation parameters in terms of a contribution through the T_{2m} term, the fit was first carried out with T_{2m} contributing to the overall relaxation (eq 2a) and second where it was set to zero (eq 2b). Application of the transverse relaxation of the bound water as a free parameter in the fitting procedure leads to larger uncertainty in the remaining fit parameters. Nevertheless, for both fitting procedures, the obtained values for the activation parameters are in good agreement.

$$\frac{1}{T_{2r}} = \frac{1}{\tau_m}\left\{\frac{T_{2m}^{-2} + (T_{2m}\tau_m)^{-1} + \Delta\omega_m^2}{(T_{2m}^{-1} + \tau_m^{-1})^2 + \Delta\omega_m^2}\right\} \quad (2a)$$

$$\frac{1}{T_{2r}} = \frac{1}{\tau_m}\left\{\frac{\Delta\omega_m^2}{\tau_m^{-2} + \Delta\omega_m^2}\right\} \quad (2b)$$

A separation of the contributing factors can be achieved by measuring their temperature dependence. For $\Delta\omega_m$, a reciprocal functionality A/T was assumed, where A was determined as a parameter in the treatment of the line-broadening data.[24] An exponential, Arrhenius-type temperature dependence was applied in the treatment of the bound-water relaxation rate $1/T_{2m}$ given by eq 3.

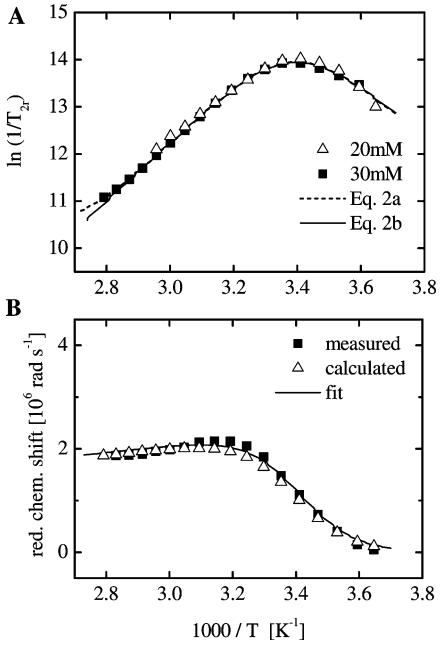

Figure 1. (**A**) Temperature dependence of the reduced transverse relaxation rate ($1/T_{2r}$) of 20 mM (△) and 30 mM (■) $[Fe^{II}(edta)(H_2O)]^{2-}$. The solid line is the result from the nonlinear fit with the reduced Swift−Connick eq 2b. The dotted line results from the fit with T_{2m} contribution represented by eq 2a. (**B**) Temperature dependence of the reduced chemical-shift difference ($\Delta\omega_r$) of the ^{17}O NMR resonance for 100 mM $[Fe^{II}(edta)(H_2O)]^{2-}$ (■) and the calculated $\Delta\omega_r$ (△) from the parameters derived in the temperature-dependent measurement of the reduced transverse relaxation rate (Table 1, column **2b**). The solid line is the fit to the measured data (■). The obtained activation parameters (Table 1, column **3**) confirm the values of the line-broadening study.

$$\frac{1}{T_{2m}} = \frac{1}{T_{2m}^0}\exp\left\{\frac{E_m}{RT}\right\} \quad (3)$$

The dependence of the exchange-rate constant (k_{ex}) on temperature variation can be derived from the Eyring equation. Here, the reciprocal residence time, k_{ex}, depends on the activation parameters for the water-exchange process, namely the activation enthalpy, $\Delta H^{\neq}$, and activation entropy, $\Delta S^{\neq}$.

$$k_{ex} = \frac{1}{\tau_m} = \left(\frac{k_B T}{h}\right)\exp\left\{\left(\frac{\Delta S^{\neq}}{R}\right) - \left(\frac{\Delta H^{\neq}}{RT}\right)\right\} \quad (4)$$

A nonlinear least-squares fit of the measured data with eqs 2a and 2b, employing the expressions for the temperature dependence of $1/T_{2m}$ (eq 3) and k_{ex} (eq 4) is shown in Figure 1A. The solid curve was derived from fitting the data of a sample with a total concentration of 20 mM $[Fe^{II}(edta)(H_2O)]^{2-}$ and neglecting any T_{2m} contribution. In a second experiment, a more-concentrated complex solution (30 mM) was measured up to 358.2 K, which showed the start of a T_{2m} contribution at the highest two temperatures. This is evident from a positive deviation of the data points from the fitted curve at 353.2 and 358.2 K. Therefore, a mathematical treatment involving T_{2m} was applied (eq 2b) and resulted in the fit shown by the dotted line. In addition, the reduced

(24) Bloembergen, N. *J. Chem. Phys.* **1957**, *27*, 595.

Table 1. Activation Parameters Derived from the Least-Squares Fit of $1/T_{2r}$ as a Function of Temperature[a]

	1	**2a**	**2b**	**3**
Experimental Technique	Line-Broadening	Line-Broadening	Line-Broadening	Shift-Analysis
A	$(6.8 \pm 0.4) \times 10^8$	$(6.7 \pm 0.2) \times 10^8$	$(6.7 \pm 0.3) \times 10^8$	$(6.8 \pm 0.1) \times 10^8$
$1/T_{2m}^{298}$ (s^{-1})		$(2 \pm 38) \times 10^{13}$		
E_m (kJ mol^{-1})		-64 ± 69		
$\Delta H^{\neq}$ (kJ mol^{-1})	43 ± 2	43 ± 1	43.2 ± 0.5	43 ± 5
$\Delta S^{\neq}$ (J K^{-1} mol^{-1})	$+24 \pm 8$	$+24 \pm 5$	$+23 \pm 2$	$+25 \pm 17$
k_{ex}, 298.2K (s^{-1})	$(2.7 \pm 0.4) \times 10^6$	$(2.8 \pm 0.2) \times 10^6$	$(2.7 \pm 0.1) \times 10^6$	$(3.1 \pm 0.2) \times 10^6$

[a] Measurements at two different concentrations, 20 mM (**1**) and 30 mM (**2**), of $[Fe^{II}(edta)(H_2O)]^{2-}$ yielded parameters that are in excellent agreement. Fitting the data by including an initial T_{2m} contribution (**2a**) leads to lower accuracy compared to calculations without T_{2m} (**2b**). The fitting of the temperature dependence of $\Delta\omega_r$ for a 100 mM $[Fe^{II}(edta)(H_2O)]^{2-}$ solution yielded matching parameters (**3**).

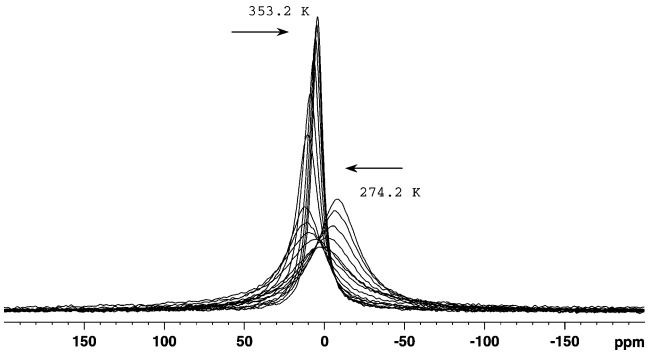

Figure 2. Shift and line-broadening of the ^{17}O resonance of a 100 mM $[Fe^{II}(edta)(H_2O)]^{2-}$ solution with temperature variation from 274.2 to 353.2 K. At low temperatures, the ^{17}O resonance shifts with increasing temperature to a lower field and the line width increases. At higher temperatures (T > 313.2 K), the resonance shifts linearly with the temperature to higher fields, and the line width decreases.

Swift−Connick equation 2a was applied for the data of the more-concentrated sample as well. The obtained curve equals that of the less-concentrated solution. All of the parameters that were determined in the described fitting procedures are given in Table 1. The obtained parameters for different total concentrations of $[Fe^{II}(edta)H_2O]^{2-}$ agree well. Setting T_{2m} as a free parameter in the fit with eq 2a resulted in a lower accuracy for the values of the activation parameters compared to those of the fit procedure neglecting T_{2m} (eq 2b). However, except for the larger errors, the absolute values for the derived parameters remain the same.

To further substantiate the activation parameters derived from the line-broadening analysis, it is advisable to study the shift of the bulk-water ^{17}O resonance as a function of temperature (Figure 2). To carry out this temperature-dependent shift measurement with an acceptable signal-to-noise ratio, a more-concentrated sample (100 mM) was recommended for the measurements in the spherical tube.

Although the higher concentration improves the observed signal, the resonance shift was never determined in a simple peak picking procedure. Instead, the ^{17}O resonances were fitted at each adjusted temperature with a Lorentzian function to give the accurate signal position. The reduced chemical-shift difference, $\Delta\omega_r$, was calculated from the observed chemical shifts of the 100 mM $[Fe^{II}(edta)(H_2O)]^{2-}$ solution, ω_{obs}, and the aqueous reference without the paramagnetic compound, ω_0, and normalized by the mole fraction of bound water P_m. The relationship between $\Delta\omega_r$ and T_{2m}, chemical shift ($\Delta\omega_m$, $\Delta\omega_{os}$), and residence time (τ_m) is given by eq 5. Analogous to the line-broadening experiment, these contributions can be separated by measuring their temperature dependences.

$$\Delta\omega_r = \frac{1}{P_m}(\omega_{obs} - \omega_0) = \frac{\Delta\omega_m}{(1 + \tau_m T_{2m}^{-1})^2 + \tau_m^2 \Delta\omega_m^2} + \Delta\omega_{os} \quad (5)$$

Figure 1B shows the measured reduced chemical shift as a function of temperature. A contribution of $\Delta\omega_{os}$ to $\Delta\omega_r$ at low temperature was never taken into consideration. With increasing temperature a strong increase in $\Delta\omega_r$ is obvious. This is a typical behavior of the chemical shift in the slow and reasonably fast exchange region. At temperatures higher than 313.2 K, the chemical-shift difference no longer increases but decreases. A changeover to the fast exchange region is evident. The observed $\Delta\omega_r$ in the temperature range for very fast exchange is dominated by the shift difference between bound and bulk water, $\Delta\omega_m$. The inflection point in the plot of $\Delta\omega_r$ and the maxima of $\ln(1/T_{2r})$ were found to be at the same temperature. Both techniques show clearly and correspondingly the proposed changeover in dominating contributions and prove the exchange phenomena independently. Applying the expressions for the temperature dependence of T_{2m}, τ_m, and $\Delta\omega_m$ in eq 5 allows for the calculation of the activation parameters and the exchange-rate constant k_{ex}. The resulting curve from the fit through the data points is shown by the solid line in Figure 1B, and the obtained activation parameters are given in Table 1 (**3**). A comparison of the values derived from the line-broadening technique with that obtained in the shift analysis shows good agreement between the different approaches. Improved accuracy seems to be an advantage of the line-broadening experiment, particularly in determining the value of the activation entropy. To evaluate the derived activation parameters from both experiments, a simulation of the temperature-dependent shift of $\Delta\omega_r$ from the data of the line-broadening experiment was also performed. The derived parameters $\Delta\omega_m$, T_{2m} and τ_m for the line-broadening experiment and their known dependence on temperature were used to calculate the reduced shift, $\Delta\omega_r$, of the ^{17}O resonance according to eq 5. A comparison of the calculated (Δ) and measured (■) shift difference $\Delta\omega_r$ is given in Figure 1B. The calculated reduced shift, $\Delta\omega_r$, from the line-broadening experiment and the fit of the measured shift data agree well. The reason for the larger error limits of the estimated activation parameters derived from the shift analysis results from the small deviation of a few data points in the intermediate temperature range of the fit. Obviously, only three measured values are slightly too large. However, a shift analysis can be performed successfully also on broadened bulk-water peaks, but small deviations in the location of the signal position have to be considered to contribute to a lower accuracy in the case of broad signals.

At higher temperatures, $\Delta\omega_r$ is dominated by the chemical shift of the bound water molecules. The significant factor for $\Delta\omega_m$ is the hyperfine coupling between the Fe^{II} electron spin and the ^{17}O nucleus. The coupling constant (A/h) serves as a proportional factor and defines the relationship between temperature variation and chemical shift of the bound water molecule. Eq 6 gives the full mathematical treatment that is necessary to derive the scalar coupling constant from variable-temperature measurement of the chemical shift for the ^{17}O nucleus.

$$\Delta\omega_m = \frac{g_L \mu_B S(S+1)B}{3k_B T}\left(\frac{A}{h}\right) \tag{6}$$

For the $Fe^{II}-O$ interaction, (A/h) was found to be 10.4 MHz. This value is close to that obtained for the coupling constant (A/h) for the $Fe^{II}-O$ interaction in the hexa-aqua complex of Fe^{2+}. Ducommun et al.[25] reported a value of 9.4 MHz for the coupling constant of aquated Fe^{II}. Unpaired electrons in the d orbitals of the iron center cause a large contact shift of the ^{17}O nucleus because of a sizable spin delocalization occurring through metal−oxygen σ bonding onto the water molecule moiety directly bound to the paramagnetic Fe^{II} center. The value of (A/h) is a measure of the overlap of unpaired spin density with the ^{17}O nucleus. In the studied system, the mechanism of spin delocalization seems to be quite insensitive to chelation. This finding corresponds to the work on the $[Mn^{II}(edta)(H_2O)]^{2-}$ system done by Hunt et al.[26] In that study, a slightly larger value (A/h) = 6.04 MHz for the chelate complex compared to 5.62 MHz for the hexa-aqua species was reported. In a later report,[27] Hunt observed the same value for the hyperfine coupling constant for Mn^{II}-*o*-phenylenediaminetetraacetate (Mn^{II}-Phdta), namely, A/h = 6.04 MHz. Furthermore, this consistency in A/h was also reported by Rablen et al.[28] for Ni^{II} complexes with the chelates diethylenetriamine (dien), triethylenetetramine (trien), and tetraethylenepentamine (tetren). The scalar coupling constants for the complexes $[Ni^{II}(dien)(H_2O)_3]^{2+}$ (22.7 MHz), $[Ni^{II}(trien)(H_2O)_2]^{2+}$ (22.5 MHz), and $[Ni^{II}(tetren)(H_2O)]^{2+}$ (25.2 MHz) are similar to that of the hexa-aqua species $[Ni^{II}(H_2O)_6]^{2+}$ (21.6 MHz). No substantial effect on the spin-delocalization process between the metal center and the ^{17}O nucleus of a bound water molecule was found for chelation of Fe^{II} by the edta ligand in $[Fe^{II}(edta)(H_2O)]^{2-}$, in agreement with the analogous spectator ligands in the above-mentioned ternary complexes.

Conclusions on the nature of the water-exchange mechanism on the basis of data from temperature-dependent measurements are limited. A dissociatively activated interchange mechanism can be suggested on the basis of the small and positive activation entropy, although conclusions based on this parameter only are, in principle, vague. To clarify the detailed mechanism of the exchange process unambiguously, k_{ex} was measured as a function of pressure as shown in Figure 3. A study of the pressure dependence is principally advisable in the slow-exchange domain (II), because $1/T_{2r} \approx k_{ex}$. However, from the temperature dependence, it is obvious that region II is not fully accessible in the available temperature range. Therefore, the experiment was performed by measuring the reduced transverse relaxation rate at different pressures at a constant temperature of 318.2 K. For the investigated system, a linear segment close to the maximum in the plot of $\ln(1/T_{2r})$ versus $1/T$ in Figure 1A belongs to the selected temperature. In this temperature region (III, fast exchange region), the Swift−Connick equation is approximated by expression 7.

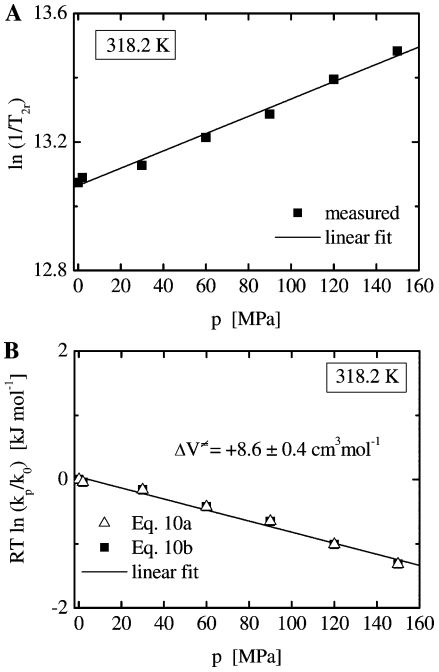

Figure 3. (**A**) Pressure dependence of the reduced transverse relaxation rate of a 30 mM $[Fe^{II}(edta)(H_2O)]^{2-}$ solution (■). (**B**) The pressure dependence of the calculated water-exchange rate constant, k_{ex}, shows similar results for both mathematical treatments (eqs 10a and 10b). The activation volume for the water-exchange process from a linear fit of the data (solid line) was determined to be $+8.6 \pm 0.4$ cm^3 mol^{-1}.

$$\frac{1}{T_{2r}} \cong \tau_m \Delta\omega_m{}^2 \tag{7}$$

A dependence of $1/T_{2r}$ and k_{ex} on pressure exists at that temperature, so that the observed increase in the transverse relaxation rate with pressure is caused by a decrease in the water-exchange rate. The relationship between the applied pressure and the exchange-rate constant at a fixed temperature T is described by eq 8.[29−31]

$$\left(\frac{\partial \ln(k)}{\partial p}\right)_T = -\frac{\Delta V^{\neq}}{RT} \tag{8}$$

The volume of activation, $\Delta V^{\neq}$, is defined as the difference between the partial molar volumes of the transition and

(25) Ducommun, Y.; Newman, K. E.; Merbach, A. E. *Inorg. Chem.* **1980**, *19*, 3696.
(26) Zetter, M. S.; Grant, M. W.; Wood, E. J.; Dodgen, H. W.; Hunt, J. P. *Inorg. Chem.* **1972**, *11*, 2701.
(27) Liu, G.; Dodgen, H. W.; Hunt, J. P. *Inorg. Chem.* **1977**, *16*, 2652.
(28) Rablen, D. P.; Dodgen, H. W.; Hunt, J. P. *Inorg. Chem.* **1976**, *15*, 931.
(29) Whalley, E. *Adv. Phys. Org. Chem.* **1964**, *2*, 93.
(30) Eckert, C. A. *Annu. Rev. Phys. Chem.* **1972**, *23*, 239.
(31) Stranks, D. R. *Pure Appl. Chem.* **1974**, *38*, 303.

reactant states. In the case of a pressure dependence of $\Delta V^{\neq}$, eq 9 is an approximate solution for the differential equation given above.

$$\ln k_p = \ln k_0 - \frac{\Delta V_0^{\neq} P}{RT} + \frac{\Delta \beta^{\neq} P^2}{2RT} \quad (9)$$

In eq 9, k_p and k_0 represent the rate constants for the observed reaction at pressure P and zero pressure, respectively. $\Delta V_0^{\neq}$ is the activation volume at zero pressure and temperature T, and $\Delta\beta^{\neq}$ is the compressibility coefficient of activation. The exchange-rate constants at different pressures k_p were obtained as solutions to both the full- and the reduced-Swift−Connick equations 2a and 2b, which are quadratic functions with respect to k_{ex}.

$$(T_{2r}^{-1} - T_{2m}^{-1})k_{ex}^2 - (2T_{2r}^{-1}T_{2m}^{-1} - T_{2m}^{-2} - \Delta\omega_m^2)k_{ex} + (T_{2m}^{-2} + \Delta\omega_m^2)T_{2r}^{-1} = 0 \quad (10a)$$

$$T_{2r}^{-1}k_{ex}^2 - \Delta\omega_m^2 k_{ex} + T_{2r}^{-1}\Delta\omega_m^2 = 0 \quad (10b)$$

In Figure 3B, the pressure dependence of k_{ex} calculated with eq 10a under consideration of $T_{2m}(\Delta)$ and with eq 10b on neglecting T_{2m} (■) resulted in matching curves. At 318.2 K, a consideration of the T_{2m} contribution does not alter the value of the rate constant significantly. As expected for a solvent with a high degree of electrostriction, the quadratic term that accounts for the compressibility of the solvent is small compared to the linear one.[32] Accordingly, this water-exchange study shows a linear behavior of $\ln(k_p/k_0)$ versus pressure, with no recognizable deviation from the linear fit (Figure 3B). Therefore, the assumption that $\Delta\beta^{\neq} = 0$ and $\Delta V^{\neq} \approx \Delta V_0^{\neq}$ is justified under the applied experimental conditions for pressures up to 150 MPa.

The values of the activation volume and the exchange-rate constant were determined to be $\Delta V^{\neq} = +8.6 \pm 0.4$ cm^3 mol^{-1} (see Table 4) and $k_{ex} = (8.9 \pm 0.1) \times 10^6$ s^{-1} (318.2 K), respectively. An evaluation of the quality of the parameter k_{ex} was achieved by comparing the obtained values from the pressure dependence, $k_{ex,p} = (8.9 \pm 0.1) \times 10^6$ s^{-1}, and temperature dependence $k_{ex,T} = (8.8 \pm 0.1) \times 10^6$ s^{-1}, at 318.2 K. The value of $k_{ex,T}$ was extrapolated to the temperature of the pressure-dependence study and shows excellent agreement.

The value of the activation volume for the water-exchange reaction is positive but considerably less than that expected for a limiting D mechanism. Nevertheless, the water-exchange reaction at the Fe^{II} center encapsulated by the edta ligand proceeds via a significantly enlarged transition state. The intimate mechanism is unambiguously identified as a dissociatively activated interchange (I_d) process with substantial bond weakening of the coordinated water molecule. Supported by a moderate positive value for the activation entropy of $+23 \pm 2$ J K^{-1} mol^{-1}, which is expected for that type of mechanism, the mechanistic course along the reaction coordinate proceeds via a transition state characterized by weak bonding to the leaving and entering water molecules.

Solution Dynamics. The ^{1}H NMR spectrum of high-spin $[Fe^{II}(edta)(H_2O)]^{2-}$ consists of broad and contact-shifted resonances characteristic for paramagnetic substances. Despite the enhanced relaxation due to the Fe^{II} center, acceptable signals were obtained in ^{1}H and ^{13}C NMR experiments. The very fast relaxation of the analogous trivalent $[Fe^{III}(edta)(H_2O)]^-$ complex causes line broadening in ^{1}H and ^{13}C NMR spectra to such an extent that no corresponding signals can be detected. In Figure 4, the ^{1}H NMR spectrum of $[Fe^{II}(edta)(H_2O)]^{2-}$ recorded at 298.2 K is shown. Two resonances at a low field with equal intensity at 74.54 and 33.11 ppm referenced to 3-(trimethylsilyl) propionic acid (TSP) were found. A closer inspection of the spectrum showed a third broadened peak near to the water signal. Integration of the two downfield resonances revealed a ratio of 1:1. The integration of the peak at a higher field was attempted but was not successful because of the excessive broadening and overlap with the water signal. At elevated temperatures, this third peak at the higher field appears more sharpened and separated from the water signal. The spectra actually consist of three peaks with relative intensities of approximately 1:1:1. The ^{1}H NMR spectra of $[Fe^{II}(edta)(H_2O)]^{2-}$ in the temperature range from 278.2 to 348.2 K indicate that the signal for the ethylene backbone protons becomes observable above 308.2 K (Figure 4, left).

To account for the ^{1}H NMR spectra of $[Fe^{II}(edta)(H_2O)]^{2-}$, a comparison with the $[Co^{II}(edta)(H_2O)]^{2-}$ system is helpful. It is known from the work by Matwiyoff and Strouse[33] that Co^{II}−edta is stereochemically nonrigid. Conformationally different protons of the ethylene backbone and acetate arms experience large chemical shifts from the delocalization of spin density from the unpaired metal d electrons. A strong dependence of the contact shift on the dihedral angle results in nonequivalent equatorial and axial positions. The spectra can be expected to consist of six resonances, namely equatorial and axial positions of the IP and OP methylene protons should give rise to four signals, and the equatorial and axial ethylene protons should give rise to two signals if signal averaging due to a fast acetate interchange is not favored. Therefore, the observed three-proton resonances indicate that a Δ,Λ isomerization is operative in the case of $[Fe^{II}(edta)(H_2O)]^{2-}$. The published data of Evilia and Everhart[20] for the $[Co^{II}(edta)(H_2O)]^{2-}$ complex shows the same resonance pattern (Table 2). At 34 °C, a proton spectrum was reported that revealed two distinct resonances with relative intensities of 1:2. At higher temperature, it was found that the resonance at the higher field splits. So, the resonance at 7 ppm consists in fact of two peaks with equal intensity. At room temperature, this was obscured because of a coincidental equivalency of the chemical shift for the protons of the ethylene backbone as well as for the two equatorial out-of-plane (2 OP *eq* OAc) and axial in-plane (2 IP *ax* OAc) methylene glycinate protons.

(32) van Eldik, R. *Inorganic High-Pressure Chemistry*; van Eldik, R., Ed.; Elsevier: Amsterdam, The Netherlands, 1986; p 1.

(33) Matwiyoff, N. A.; Strouse, C. E. *J. Am. Chem. Soc.* **1970**, *92*, 5222.

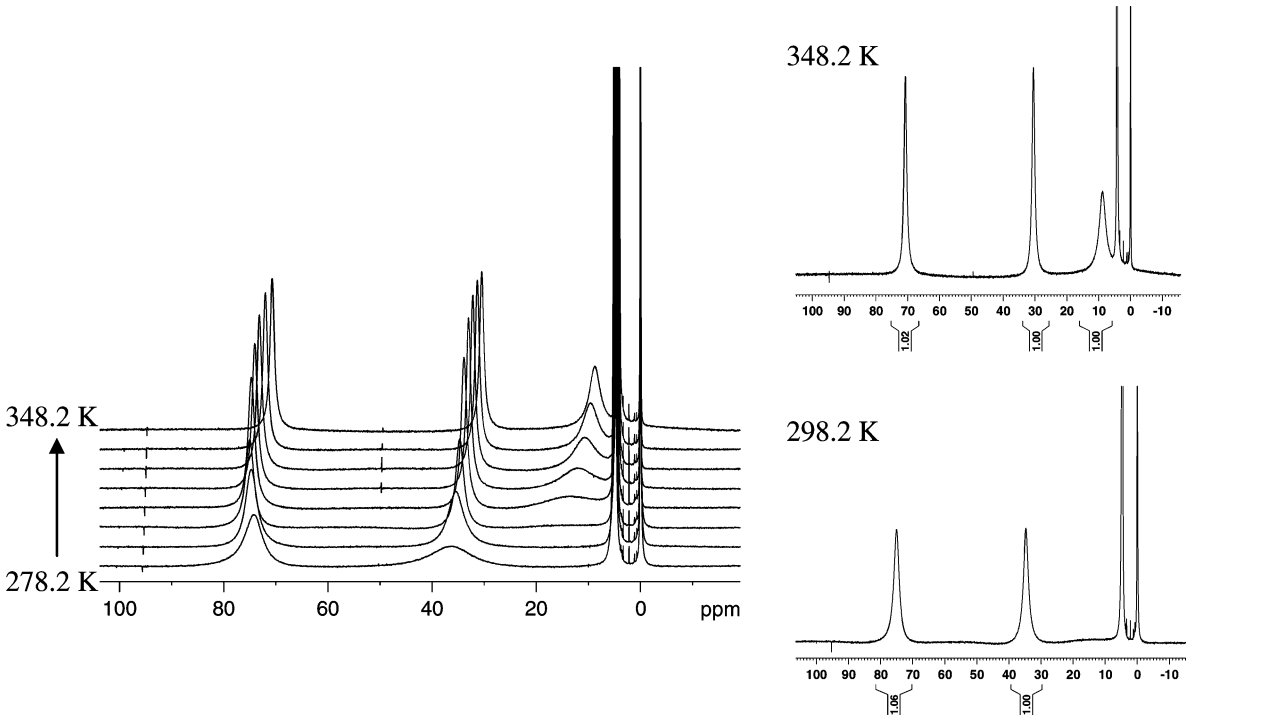

Figure 4. Left: Temperature dependence of the ^{1}H NMR spectra for paramagnetic high-spin $[Fe^{II}(edta)(H_2O)]^{2-}$. The magnetically nonequivalent axial (*ax*) and equatorial (*eq*) protons of the glycinate methylene protons lead to two distinct resonances shifted to low field. Right: Integrated ^{1}H NMR spectra of the paramagnetic high-spin $[Fe^{II}(edta)(H_2O)]^{2-}$ at 298.2 and 348.2 K, respectively.

Table 2. ^{1}H NMR Signals of Paramagnetic Co^{II}−edta and Fe^{II}−edta Complexes[a]

Co^{II}−edta[20]		Fe^{II}−edta		
shift (ppm)	assignment	shift (ppm)	rel. int.	assignment
128	2OP *ax* OAc + 2IP *eq* OAc	74.54	1.02	2OP *ax* OAc + 2IP *eq* OAc
7	2OP *eq* OAc + 2IP *ax* OAc	33.11	1.00	2OP *eq* OAc + 2IP *ax* OAc
7	4en	15.18	1.00	4en

[a] The assignment of the resonances is based on published data for the analogous cobalt complex.

The spectroscopic observations can satisfactorily be explained by a Δ,Λ-isomerization process that is of the twist-type mechanism. Neither a metal−nitrogen bond rupture nor a dechelation of a carboxylate group is required in this process. An averaging of IP and OP resonances by a nitrogen-inversion process can be ruled out to be operative in the discussed system because it does not lead to the observed, averaged-backbone resonances and requires an unfavorable metal−nitrogen bond rupture (Figure 5). The exchange between IP and OP positions of the acetate arms (Δ,Λ isomerization) leads to the observed equivalency of the glycinate methylene groups, but their protons in axial (H_{ax}) and equatorial (H_{eq}) positions remain magnetically inequivalent, caused by the long-lived nitrogen−metal bond compared to the NMR time scale.[34]

To further substantiate the findings of the ^{1}H NMR study, the ^{13}C NMR spectrum of $[Fe^{II}(edta)(H_2O)]^{2-}$ was recorded. It revealed two resonances at −232.35 and −301.96 ppm with relative intensities of 1:2. The observed equivalency

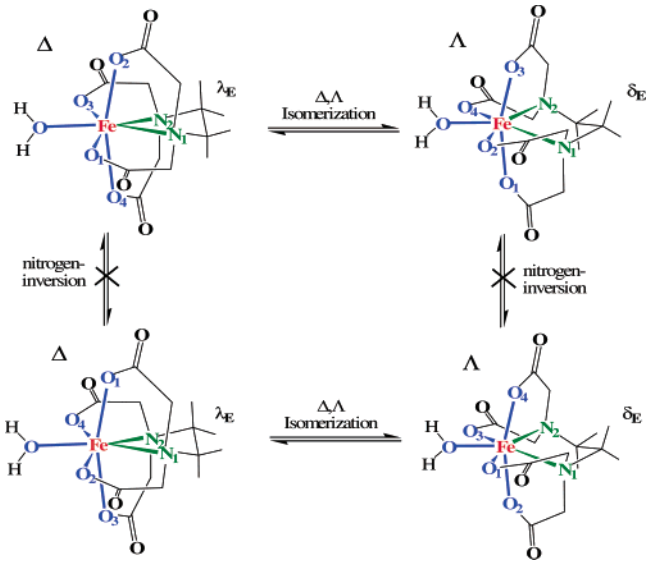

Figure 5. Δ,Λ isomerization of $[Fe^{II}(edta)(H_2O)]^{2-}$. The exchange of the glycinate rings between IP and OP positions via a pseudorotational pathway leads to a single, time-averaged signal for the protons of the ethylene backbone (axial and equatorial positions of the protons are symbolized by the orientation of the lines). Fast enantiomerization averages the methylene groups of the glycinate rings as well. The protons of these methylene groups remain magnetically inequivalent during this process.

for the carbon atoms of the ethylene backbone and the glycinate methylenes supports the observations of the ^{1}H NMR study. The Δ,Λ-isomerization process averages the resonance for the carboxylate carbons so that one peak at 187.31 ppm remains. Similar observations can be found in the literature, for example Anderegg et al. reported a ^{13}C NMR study[35] on a Tl^{III}−edta complex, in which the four carboxylate carbons appear equivalent, shifted downfield to

(34) Erickson, L. E.; Young, D. C.; Ho, F. F.-L.; Watkins, S. R.; Terrill, J. B.; Reilley, C. N. *Inorg. Chem.* **1971**, *10*, 441.

$\delta = 175.4$ ppm. A singlet for all of the glycinate methylene carbons at $\delta = 58.0$ ppm and a doublet for the ethylene backbone carbons at $\delta = 51.7$ ppm, $J(Tl, {}^{13}C) = 157$ Hz, indicate the observation of a Δ,Λ-isomerization process for this system. Howarth and co-workers noted the same kind of fluxional behavior in the case of Pb^{II}−edta ($\delta =$ 180.0 ppm), Zn^{II}−edta ($\delta = 179.9$ ppm), Cd^{II}−edta ($\delta =$ 179.4 ppm), and Hg^{II}−edta ($\delta = 177.4$ ppm) by observing only one ^{13}C signal for the carboxyl carbons.[36]

Further investigations that were performed on the solution dynamics of the nitrosyl complex $[Fe^{III}(edta)(NO^-)]^{2-}$ showed that signal averaging still occurs in this system. In Table 3, the observed proton and carbon resonances for $[Fe^{III}(edta)(NO^-)]^{2-}$ are shown together with those for $[Fe^{II}(edta)(H_2O)]^{2-}$. A comparison of the shift pattern for both complexes reveals undoubtedly that the rearrangement of the edta ligand that changes the absolute configuration is not prevented when NO occupies the seventh coordination site instead of water.

In our investigations, both ternary complexes $[Fe^{II}(edta)(H_2O)]^{2-}$ and $[Fe^{III}(edta)(NO^-)]^{2-}$ do not adopt a static structure in solution but undergo a fast rearrangement of the chelate ligand. The spectroscopic observations in solution clearly indicate a rapid acetate-scrambling process for $[Fe^{II}(edta)(H_2O)]^{2-}$ and $[Fe^{III}(edta)(NO^-)]^{2-}$ that changes the absolute configuration of both complexes (Δ,Λ isomerization).

Mechanistic Discussion. The presented data for the water-exchange process on $[Fe^{II}(edta)(H_2O)]^{2-}$ are the first available kinetic results for the family of highly oxygen-sensitive aminopolycarboxylate complexes of Fe^{II}. Therefore, the discussion is restricted to a limited series of available data, namely, aquated $Fe^{II/III}$, edta complexes of $Fe^{II/III}$, and complexes of edta-type ligands with other metal centers. The effect of the edta spectator ligand on the water-exchange kinetics and the mechanism can be evaluated by comparing the water-exchange process for the chelated complex to that of fully aquated Fe^{II}. As outlined in several studies, chelation by ligands such as edta should alter the lability of the remaining water molecules profoundly. Two factors that contribute to the water-exchange kinetics have to be discussed. First, the steric constraints around the metal center and second, the electron-donating or -withdrawing properties of the chelate ligand. For polyamines, a proportionality between the number of nitrogen donors and the lability of the water molecule was found for Ni^{2+} complexes. These observations have been ascribed to the σ-donating properties of the bound amines.[37] The electron donation toward the metal center reduces the effective charge on the nucleus. However, similar values for k_{ex} were found for the complexes $[Ni^{II}(bpy)(H_2O)_4]^{2+}$, $[Ni^{II}(bpy)_2(H_2O)_2]^{2+}$, and $[Ni^{II}(tpy)(H_2O)_3]^{2+}$. The modest change in lability was ascribed to the appearance of additional electron-withdrawing effects through the π-bonding system.[38] Unfortunately, the mechanistic course was not clarified by a pressure-dependence study on k_{ex}, which makes it difficult to evaluate the effect of steric hindrance on k_{ex} because of the space required by the spectator ligands.

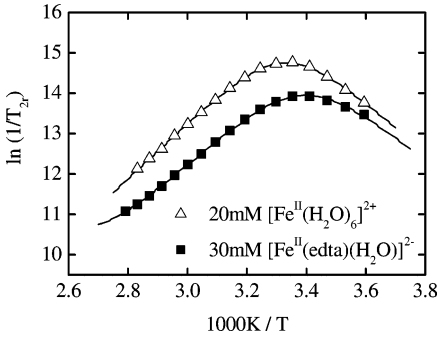

Figure 6. Temperature dependence of the reduced transverse relaxation rate ($1/T_{2r}$) of 30 mM (■) $[Fe^{II}(edta)(H_2O)]^{2-}$ and 20 mM $[Fe^{II}(H_2O)_6]^{2+}$ (△) at pH 5.0. The solid lines are the result from the nonlinear fit with the reduced Swift−Connick equation.

Table 3. ^1H and ^{13}C NMR Signals of the Paramagnetic $[Fe^{II}(edta)(H_2O)]^{2-}$ and $[Fe^{III}(edta)(NO^-)]^{2-}$ Complexes

$[Fe^{II}(edta)(H_2O)]^{2-}$		$[Fe^{III}(edta)(N^-)]^{2-}$	
^1H shift (ppm)	assignment	^1H shift (ppm)	assignment
74.54	2OP *ax* OAc + 2IP *eq* OAc	51.32	2OP *ax* OAc + 2IP *eq* OAc
33.11	2OP *eq* OAc + 2IP *ax* OAc	36.84	2OP *eq* OAc + 2IP *ax* OAc
15.18	4en	21.4	4en
^{13}C shift (ppm)	assignment	^{13}C shift (ppm)	assignment
187.31	$-COO^-$	184.24	$-COO^-$
−232.35	$-NCH_2CH_2N-$	−243.11	$-NCH_2CH_2N-$
−301.96	$-CH_2COO^-$	−313.77	$-CH_2COO^-$

To evaluate the electronic and steric influence of the edta ligand on the water-exchange reaction, we studied the exchange kinetics for $[Fe^{II}(edta)(H_2O)]^{2-}$ as a function of temperature and pressure and compared the data with the kinetics for the fully aquated species $[Fe^{II}(H_2O)_6]^{2+}$ studied under the same experimental conditions (Figure 6).

The obtained parameters are listed in Table 4 and how values for the aquated-Fe^{II} species similar to those reported by Ducommun et al.[25] in acidified solutions (60% $HClO_4$).

A comparison of the obtained values of k_{ex} for the aquated-Fe^{II} species (columns **2a** and **2b** of Table 4) and the chelate complex (Table 4, column **1**) reveals a slightly slower water-exchange reaction for the edta-chelated Fe^{II} complex. The activation volume of $+8.6$ cm^3 mol^{-1} indicates larger bond weakening in the case of $[Fe^{II}(edta)(H_2O)]^{2-}$ as compared to the value of $+4.1$ cm^3 mol^{-1} for $[Fe^{II}(H_2O)_6]^{2+}$ (Figure 7). Nevertheless, the exchange rate is slowed down by a factor of 1.6. One reason for this finding might be a disfavored attack of the entering water molecule caused by increased steric constraints around the metal center in the

(35) Anderegg, G.; Popov, K.; Pregosin, P. S. *Magn. Reson. Chem.* **1987**, *25*, 84.
(36) Howarth, O. W.; Moore, P.; Winterton, N. *J. Chem. Soc., Dalton Trans.* **1974**, 2271.
(37) Hunt, J. P. *Coord. Chem. Rev.* **1971**, *7*, 1.
(38) Grant, M.; Dodgen, H. W.; Hunt, J. P. *J. Am. Chem. Soc.* **1970**, *92*, 2321.
(39) Swaddle, T. W.; Merbach, A. E. *Inorg. Chem.* **1981**, *20*, 4212.
(40) Grant, M. W.; Jordan, R. B. *Inorg. Chem.* **1981**, *20*, 55.

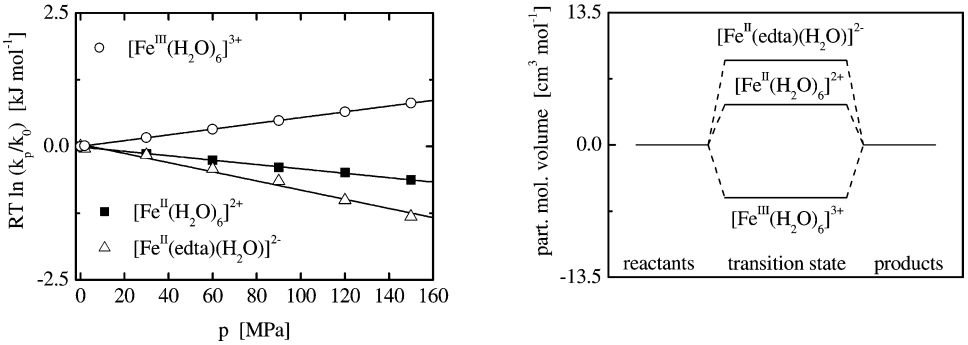

Figure 7. Left: Comparison of the pressure dependence of water exchange on $[Fe^{III}(H_2O)_6]^{3+}$ (○),[38] $[Fe^{II}(H_2O)_6]^{2+}$ (■), and $[Fe^{II}(edta)(H_2O)]^{2-}$ (△). Right: Volume profile for the water-exchange reaction with the transition-state volume following the sequence $[Fe^{III}(H_2O)_6]^{3+}$ < $[Fe^{II}(H_2O)_6]^{2+}$ < $[Fe^{II}(edta)(H_2O)]^{2-}$.

Table 4. Activation Parameters Resulting from the Least-Squares Fit of $1/T_{2r}$ as a Function of Temperature for $[Fe^{II}(edta)(H_2O)]^{2-}$ (**1**, this Work) and $[Fe^{II}(H_2O)_6]^{2+}$ (**2a**, this Work) at pH 5.0[a]

	1	**2a**	**2b**	**3**
k_{ex}, 298.2 K (s^{-1})	$(2.7 \pm 0.1) \times 10^6$	$(4.3 \pm 0.1) \times 10^6$	$(4.4 \pm 0.2) \times 10^6$	1.6×10^2
$\Delta H^{\neq}$ (kJ mol^{-1})	43.2 ± 0.5	48.2 ± 0.6	41.4 ± 1.2	64.0
$\Delta S^{\neq}$ (J mol^{-1} K^{-1})	$+23 \pm 2$	$+44 \pm 2$	$+21 \pm 5$	+12.1
$\Delta V^{\neq}$ (cm^3 mol^{-1})	$+8.6 \pm 0.4$	+4.1	+3.8	−5.4

[a] For comparison the values reported by Ducommun et al.[25] for $[Fe^{II}(H_2O)_6]^{2+}$ (**2b**) and by Swaddle and Merbach[39] and Grant and Jordan[40] for $[Fe^{III}(H_2O)_6]^{3+}$ (**3**) are shown.

Table 5. Rate and Activation Parameters for Water Exchange on $[Gd^{III}(H_2O)_8]^{3+}$ (**1**), $[Gd^{III}(pdta)(H_2O)_2]^{-}$ (**2**), $[Gd^{III}(dtpa)(H_2O)]^{2-}$ (**3**), $[Eu^{II}(H_2O)_7]^{2+}$ (**4**), and $[Eu^{II}(dtpa)(H_2O)]^{3-}$ (**5**)

	1[41]	**2**[41]	**3**[42]	**4**[43,44,45]	**5**[46]
k_{ex}, 298.2 K (s^{-1})	830×10^6	102×10^6	4.1×10^6	5000×10^6	1300×10^6
$\Delta H^{\neq}$ (kJ mol^{-1})	14.9	11.0	52.0	15.7	26.3
$\Delta S^{\neq}$ (J mol^{-1} K^{-1})	−24.1	−54.6	+56.2	−7.0	+18.3
$\Delta V^{\neq}$ (cm^3 mol^{-1})	−3.3	−1.5	+12.5	−11.3	+4.5

Fe^{II}−edta complex. Another important feature responsible for the decrease in the water-exchange velocity in the Fe^{II}−edta system certainly concerns the flexibility of the metal-coordination environment in the chelate complex as compared to the hexa-aqua ion. The metal-coordination environment can be expected to show a higher degree of elasticity for water approach and release during the dissociatively activated water exchange in the case of the hexa-aqua Fe^{II}. As a result, rearrangements of the metal-coordination environment to reach the transition state can be expected to be realized easier in $[Fe(H_2O)_6]^{2+}$ than in $[Fe(edta)(H_2O)]^{2-}$, such that the water exchange becomes slightly faster in the former case.

Analogous observations were made in studies by Merbach et al.[41−46] The reported water-exchange reactions of complexes with aminopolycarboxylate ligands were performed with Gd^{3+} and Eu^{2+} as metal ions. The complexes with the edta-related dtpa (diethylenetriaminepentaactate) and pdta (1,3-propylenediaminetetraacetate) chelates were investigated because of their potential use as contrast agents in MRI. Comparing the kinetics for the aminopolycarboxylato and aqua complexes of Gd^{3+} and Eu^{2+}, the chelate complexes were found to exchange the bound water molecule significantly slower than the aquated species (Table 5).

Our data for $[Fe^{II}(edta)(H_2O)]^{2-}$ reveal a virtually identical behavior. The water-exchange process is slowed down but only by a factor of 1.6, which is a moderate effect compared to that found on going from the fully aquated to the dtpa complexes in the case of Gd^{3+} (8.1 times slower) and Eu^{2+} (3.8 times slower). The above-mentioned hindered attack of the entering water molecule on the encapsulated Fe^{II} is also in-line with the findings for the Gd^{III} and Eu^{II} aminoploycarboxylate complexes.[41−46] Especially, the activation volumes clearly indicate the need for a considerable dissociation of the bound water molecule in the chelate complexes. The magnitude of this effect is suggested to depend on the size of the metal center and the steric constraints around the metal center as a result of the chelate ligand. The latter can, obviously, additionally be triggered by the nature of the chelate ligand. We can thus state in summary that the absolute magnitudes of k_{ex} for the water-exchange reactions of the above-mentioned aminopolycarboxylate complexes of Fe^{2+}, Gd^{3+}, and Eu^{2+} are slower than those of the corresponding metal−aqua complexes. Steric hindrance around the metal center apparently dominates over the labilizing effect of the chelates.

An accelerated water-exchange reaction due to chelation is observed, however, in the case of $[Fe^{III}(edta)(H_2O)]^{-}$, the trivalent relative of $[Fe^{II}(edta)(H_2O)]^{2-}$. The former exchanges the bound water molecule 450 000 times faster than $[Fe^{III}(H_2O)_6]^{3+}$. This tremendously enhanced exchange process is a manifestation of the combined σ- and π-donating

(41) Micskei, K.; Powell, D. H.; Helm, L.; Brücher, E.; Merbach, A. E. *Magn. Reson. Chem.* **1993**, *31*, 1011.
(42) Micskei, K.; Helm, L.; Brücher, E.; Merbach, A. E. *Inorg. Chem.* **1993**, *32*, 3844.
(43) Caravan, P.; Merbach, A. E. *Chem. Commun.* **1997**, 2147.
(44) Caravan, P.; Toth, E.; Rockenbauer, A.; Merbach, A. E. *J. Am. Chem. Soc.* **1999**, *121*, 2147.
(45) Moreau, G.; Helm, L.; Purans, J.; Merbach, A. E. *J. Phys. Chem.* **2002**, *106*, 3034.
(46) Seibig, S.; Toth, E.; Merbach, A. E. *J. Am. Chem. Soc.* **2000**, *122*, 5822.
(47) Schneppensieper, T.; Seibig, S.; Zahl, A.; Tregloan, P.; van Eldik, R. *Inorg. Chem.* **2001**, *40*, 3670.

Table 6. Activation Parameters Resulting from the Least-Squares Fit of $1/T_{2r}$ as a Function of Temperature for $[Fe^{II}(edta)(H_2O)]^{2-}$ (20 mM, **1a**), (30 mM, **1b**), and $[Fe^{III}(edta)(H_2O)]^{-}$ (30 mM, **2a**) at pH 5.0[a]

	1a	1b	2a	2b
k_{ex}, 298.2K (s^{-1})	$(2.7 \pm 0.4) \times 10^6$	$(2.8 \pm 0.2) \times 10^6$	$(6.0 \pm 0.3) \times 10^7$	7.2×10^7
$\Delta H^{\neq}$ (kJ mol^{-1})	43.4 ± 2.3	43.4 ± 1.4	24.2 ± 0.6	24.3 ± 0.7
$\Delta S^{\neq}$ (J mol^{-1} K^{-1})	$+24 \pm 8$	$+24 \pm 5$	-14 ± 2	-13 ± 2
$\Delta V^{\neq}$ (cm^3 mol^{-1})		$+8.6 \pm 0.4$	$+3.6 \pm 0.1$	$+2.2 \pm 0.3$

[a] For comparison, values reported by Schneppensieper et al.[47] for $[Fe^{III}(edta)(H_2O)]^{-}$ at pH 3.9 (**2b**) are shown.

properties of the edta donor atoms. Binding of a metal center with a charge of 3+ to edta, where the N donors have σ- and the O donors have both σ- and π-donating properties, leads to a decreased surface-charge density in comparison to the hexa-aqua Fe^{III} ion. As a consequence of this modification, the $Fe^{III}-OH_2$ bond in $Fe^{III}-$edta is considerably weaker than in $[Fe(H_2O)_6]^{3+}$, which leads to the above-mentioned enhancement of the water-exchange reaction rate by several orders of magnitude. On the one hand, the increase in steric hindrance of the chelate skeleton toward the attacking water in the I_d process should also occur in the case $[Fe^{III}(edta)(H_2O)]^{-}$. On the other hand, this factor is apparently overcompensated by the $Fe^{III}-OH_2$ bond labilization.

Electronic and steric contributions due to the chelate ligand cannot be separated and have opposite effects on the water-exchange rate. Despite the fact that the exchangeable water molecules are confined by very similar cavities in $[Fe^{II}(edta)(H_2O)]^{2-}$ and $[Fe^{III}(edta)(H_2O)]^{-}$, the different steric constraints can nevertheless be identified on the basis of the trend in the $\Delta V^{\#}$ values. Thus, the participation of the entering water molecule is less favored in the case of both metal chelates as compared to the hexa-aqua complexes. The mechanism for the exchange reaction needs to proceed via a dissociatively activated interchange process. Indeed, a changeover in mechanism from associatively to dissociatively activated interchange was found on going from $[Fe^{III}(H_2O)_6]^{3+}$ ($\Delta V^{\neq} = -5.4$ cm^3 mol^{-1})[39,40] to the chelated species $[Fe^{III}(edta)(H_2O)]^{-}$ ($\Delta V^{\neq} = +3.6$ cm^3 mol^{-1}).

The difference between the trivalent and divalent iron complexes becomes evident from all of the kinetic and mechanistic differences described above (Table 6). This difference should be largely caused by the different d-electron configurations. The absence of ligand-field-stabilization effects in high-spin $[Fe^{III}(edta)(H_2O)]^{-}$ ($t_{2g}^3e_g^2$) with a spherically symmetric electron cloud should lead to an enhanced flexibility of the whole system. Flexibility and the ease of elongation of the chelate-bite distance play an important role when conformational changes are required during the water-exchange process. The studies on the solution dynamics of $[Fe^{II}(edta)(H_2O)]^{2-}$ revealed a Δ,Λ-isomerization process that exchanges the carboxylate groups between IP and OP environments, but the nitrogen bonds need to be considered as long-lived. Therefore, the observed dynamic isomerization does not lead to flexibility on the basis of bond-length changes and changes in the chelate-bite distance, which is energetically disfavored in the divalent iron complexes. The coordination cage of the edta ligand in the $[Fe^{II}(edta)(H_2O)]^{2-}$ complex remains rigid with respect to the size of the open site, where the water-exchange process occurs. As a result, the exchange reaction in the case of heptacoordinate $[Fe^{II}(edta)(H_2O)]^{2-}$ necessarily has to proceed via a considerable dissociatively activated exchange process with a larger positive activation volume of $+8.6 \pm 0.4$ cm^3 mol^{-1}. In the case of the trivalent edta complex, the smaller activation volume ($+3.6$ cm^3 mol^{-1}) indicates a less-pronounced dissociation of the bound water molecule in the transition state. As a result of the principle of microscopic reversibility for a symmetric solvent-exchange reaction, the entering water molecule approaches closer to the metal center in the trivalent species, indicated by the smaller activation volume and therefore contributes more to the exchange rate.

Conclusions

The water-exchange reaction for the $[Fe^{II}(H_2O)_6]^{2+}$ species is faster ($k_{ex} = 4.4 \times 10^6$ s^{-1}) than for the chelated $[Fe^{II}(edta)(H_2O)]^{2-}$ complex ($k_{ex} = 2.7 \times 10^6$ s^{-1}), where steric constraints at the encapsulated Fe^{II} metal center disfavor the approach of an entering water molecule. The displacement of the bound water in $[Fe^{II}(edta)(H_2O)]^{2-}$ requires considerable bond weakening as indicated by a larger activation volume for the edta complex ($+8.6 \pm 0.4$ cm^3 mol^{-1}) as compared to a value of $+3.8$ cm^3 mol^{-1} for $[Fe^{II}(H_2O)_6]^{2+}$. The nonspherical asymmetric electronic configuration of high-spin Fe^{II} results in a reduced water-exchange rate for $[Fe^{II}(edta)(H_2O)]^{2-}$ as compared to the Fe^{III} analogue by a factor of 2.2, where ligand-field stabilization is missing and conformational changes are easily feasible. Accordingly, in the Fe^{II} case, the water-exchange reaction is slowed down as a result of increased steric hindrance by chelation and because of its nonspherical electronic configuration.

Both $[Fe^{II}(edta)(H_2O)]^{2-}$ and $[Fe^{III}(edta)(NO^{-})]^{2-}$ do not adopt a static structure in solution. The solution NMR spectra of $[Fe^{II}(edta)(H_2O)]^{2-}$ and $[Fe^{III}(edta)(NO^{-})]^{2-}$ reveal an isomerization process in solution that interchanges the IP and OP positions of the acetate arms.

Acknowledgment. The authors gratefully acknowledge financial support from the Deutsche Forschungsgemeinschaft through SFB 583 on redox-active metal complexes. R.M. is grateful to the Deutsche Forschungsgemeinschaft for Grant Me1148/7-1.

Supporting Information Available: Summary of the measured data in the ^{17}O relaxation study of the $[Fe^{II}(edta)(H_2O)]^{2-}$ complex, data for the temperature and pressure dependencies of 20 mM $[Fe^{II}(H_2O)]^{2+}$ and 30 mM $[Fe^{III}(edta)(H_2O)]^{-}$. This material is available free of charge via the Internet at http://pubs.acs.org.

IC700472Q